Acta Scientific Pharmaceutical Sciences (ISSN: 2581-5423)

Volume 8 Issue 7 July 2 024

Review Article

Optimized Structure, Spectroscopy Research, Reactive Site Analysis and Pharmaceutical Studies on Abametapir – a DFT Approach

B Aysha Rifana[1,2], Usha G[2,3], Johanan Christian Prasana[1,2]* and A Anuradha[2,3]

[1]*Department of Physics, Madras Christian College, Tamil Nadu, India*

[2] *University of Madras, Chennai, Tamil Nadu, India*

[3]*PG and Research Department of Physics, Queen Mary's College, Tamil Nadu, India*

***Corresponding Author:** Johanan Christian Prasana, Department of Physics, Madras Christian College, Tamil Nadu, India.

Received: May 31, 2024

Published: June 19, 2024

Abstract

Abametapir is a dimethyl-bipyridine that has antifungal and antiviral activity. Optimised geometry and vibrational wavenumbers of Abametapir were obtained using the DFT calculations. VEDA was used to determine the vibrational assignments for each normal mode. TD-DFT technique was used to depict the theoretical UV-visible spectrum. HOMO-LUMO and Donor-Acceptor (NBO) interactions of Abametapir were also assessed. Nucleophilic and electrophilic regions were identified using the MEP map. ELF and LOL computations were used to determine the electron locations at bonding and antibonding sites. Based on the bioactivity assessment, Abametapir demonstrates satisfactory drug-like behaviour and satisfy with Lipinski's rule. Furthermore, A significant binding affinity between the title compound and the target proteins 1P30 (Adenovirus) and 1M17(Lung cancer) was found using Molecular Docking analysis.

Keywords: Abametapir; Lung Cancer; Adenovirus

Introduction

Abametapir is a dipyridine compound with anti-fungal and anti-viral activity. Its empirical formula is $C_{12}H_{12}N_2$, and its IUPAC NAME is 5,5'-Dimethyl-2,2-dipyridal [1]. Derivatives of pyridines are important compounds with numerous biological uses. A significant portion of these compounds are shared in therapeutic applications [2]. One important heterocyclic compound that is used to treat a variety of human ailments is pyridine. It is found in many pharmaceutical products [3]. As the substituents on the pyridine nucleus change, the biological targets shift from viral issues to microbial diseases. Pyridine derivatives interact with proteins, enzymes, and DNA to target various biological issues. Pyridine includes Anti-microbial [4], Anti-fungal [5], Anti-inflammatory [6], Anti-diabetic [7], Anti-cancer [8,9], Anti-viral [10,11], Anti-oxidant activities [12].

Adenovirus are DNA virus that typically cause mild infections involving the upper or lower respiratory tract, ocular, and gastrointestinal tract [13]. Adenovirus is generally found in children's [14]. These disorders typically have minimal symptoms that are curable. In rare situations, serious disorders such as hepatitis, myocarditis, and nephritis may occur [15]. Adenovirus may also induce epidemic keratoconjunctivitis (EKC) in cases of ocular infection, which would impair visual acuity [16]. Although adenoviruses have been identified for years, no FDA-approved medicine exists to treat human adenovirus infection. Only two antiviral medications, cidofovir and ribavirin, are currently utilized in the initial stage of adenovirus treatment. In this study, an attempt is made to theoretically prove that Abametapir could be used in the treatment of adenovirus.

According to a review of the literature [17-26], no spectroscopic or molecular docking research have focused on Abametapir. As a

result, studies were conducted on Abametapir structural properties and biological roles. A thorough vibrational and electrical examination against a theoretical foundation is provided by the current work. A comprehensive spectroscopic study of Abametapir has been described using DFT theory. Abametapir reactive sites were studied with the use of MEP (Molecular Electrostatic Potential), ELF (Electron Localization Function) and LOL (Localised Orbital Locator). Molecular docking was used to ascertain Abametapir Adenovirus activity.

Computational details

DFT and TD-DFT calculations were performed using Gaussian 09W [27] software and GaussView 6 [28]. Furthermore, Chemcraft 1.8 [29] was used for data extraction and visualisation from the Gaussian calculation output. Abametapir wavenumbers were assigned by the use of VEDA 4.0 tool [30] and the PED was calculated for each mode. Investigation of the Frontier Molecular Orbitals, Natural Bond Orbital, and Molecular Electrostatic Potential was done using Gaussian 09W. Multiwfn 3.8 was used for topological research [31]. Abametapir 's pharmacological evaluation was carried out with the use of SwissADME [32], AutoDock Tools 1.5.6 [33], and Discovery Studio Visualizer [34].

Outcomes and Discussions

Bond parameters analysis

The term "Bond Parameters" describes how a covalent Bond is characterized using parameters, such as "Bond Length" and "Bond Angle". An angle between two pairs is called the Bond angle. Distance between two nearby atoms is known as the Bond length. Bond parameters (Bond length and Bond angle) of the Abametapir are derived and are listed in Table 1. Optimized molecular structure of Abametapir is shown in Figure 1. Homonuclear atoms such as C10-C13, C1-C7, C7-C8, C8-C9, C3-C4 have the highest Bond length of 1.507,1.489,1.399,1.389,1.396Å whereas the Heteronuclear atoms such as C1-N6, C5-N6, C11-N12, C7-N12 have Bond length of 1.343,1.330,1.330,1.343Å. Bond angle, the maximum values obtained were 124.5,122.6,121.8 and 121.7º which corresponds to the atoms C10-C11-N12, C9-C10-C13, C3-C2-H15, C2-C1-N6. Homonuclear atoms such as C4- C5, C10-C11 have the same Bond angle 1.401º. The atoms H12- C13- H22, H21-C13-H23, H24-C14-H25, H24- C14-H26 have the same bond angle 107.8º respectively.

BOND PARAMETERS	B3LYP/6-311++G(d,p)
Bond Length(A^0)	
C1-C2	1.399
C1-N6	1.343
C1-C7	1.489
C2-C3	1.389
C2-H15	1.081
C3-C4	1.396
C3-H16	1.086
C4-C5	1.401
C4-C14	1.507
C5-N6	1.330
C5-H17	1.089
C7-C8	1.399
C7-N12	1.343
C8-C9	1.389
C8-H18	1.081
C9-C10	1.396
C9-H19	1.086
C10-C11	1.401
C10-C13	1.507
C11-N12	1.330
C11-H20	1.089
C13-H21	1.092
C13-H22	1.094
C13-H23	1.094
C14-H24	1.092
C14-H25	1.094
C14-H26	1.094
Bond Angle(^{0})	
C2-C1-N6	121.7
C2-C1-C7	121.1
C1-C2-C3	118.9
C1-C2-H15	119.2
N6-C1-C7	117.2
C1-N6-C5	118.5
C1-C7-C8	121.1
C1-C7-N12	117.2

C3-C2-H15	121.8
C2-C3-C4	120.1
C2-C3-H16	120.0
C4-C3-H16	120.0
C3-C4-C5	116.3
C3-C4-C14)	122.6
C5-C4-C14	121.1
C4-C5-N6	124.5
C4-C5-H17	119.7
C4-C14-H24	111.2
C4-C14-H25	111.3
C4-C14-H26	111.3
N6-C5-H17	115.8
C8-C7-N12	121.7
C7-C8-C9	118.9
C7-C8-H18	119.2
C7-N12-C11	118.5
C9-C8-H18	121.8
C8-C9-C10	120.1
C8-C9-H19	120.0
C10-C9-H19	120.0
C9-C10-C11	116.3
C9-C10-C13	122.6
C11-C10-C13	121.1
C10-C11-N12	124.5
C10-C11-H20	119.7
C10-C13-H21	111.2
C10-C13-H22	111.3
C10-C13-H23	111.3
N12-C11-H20	115.8
H21-C13-H22	107.8
H21-C13-H23	107.8
H22-C13-H23	107.2
H24-C14-H25	107.8
H24-C14-H26	107.8
H25-C14-H26	107.2

Table 1: Optimized geometrical parameters of abametapir.

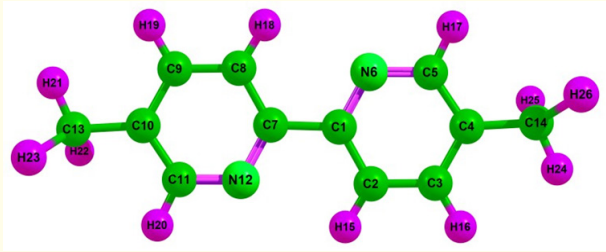

Figure 1: Optimized structure of Abametapir.

Vibrational investigation

A nonlinear molecule with N atoms has a maximum number of potential active observable fundamentals equal to (3N-6) minus the three translational and three rotational degrees of freedom. With 26 atoms, the title molecule has 72 normal modes of vibration [35]. FT-IR and FT-RAMAN theoretical spectra are shown in Figure 2 and 3. Spectral allocations of selected modes with PED contributions are tabulated in Table 2.

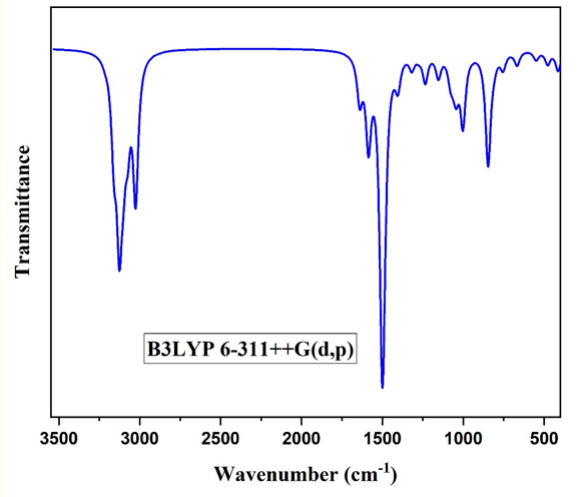

Figure 2: Theoretical FT-IR Spectrum of Abametapir.

C-H vibration

Because of the aromatic C-H stretching vibration present in Abametapir, aromatic compounds frequently have multiple weak bonds in the 3100-3000 cm-1 range [36]. C-H stretching vibrations in the current investigation were recorded at 2933-2742cm-1 with PED values of 100,99,97,92,86,78,70%. The wavelength of 2800 and 2742cm-1 has pure stretching and it is evident from the PED values of 100%.

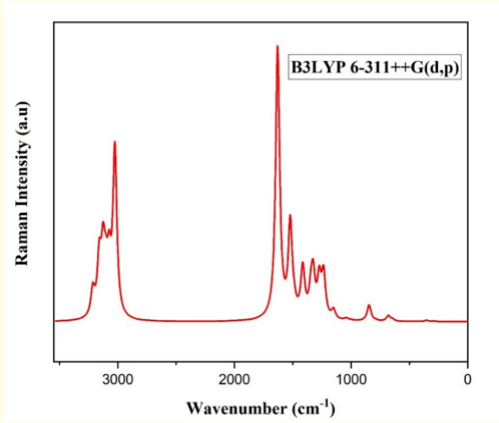

Figure 3: Theoretical FT-RAMAN Spectrum of Abametapir.

N-C vibration

N-C stretching is found at 1200-1350 cm^{-1} for aromatic amines. N-C stretching vibrations are obtained at the wavelength of 1258,1212,1056cm^{-1} with PED values of 39,42 and 20% respectively.

C-C vibration

Stretching vibrations (C=C bond) are expected in the region of 1300-1000 cm^{-1} [37]. The bands which are of different intensities were observed in the present study. C-C vibrational modes was obtained at the wavelength are 1887, 1589, 1565, 1554, 1258, 1215, 1018, 1013, 790, 696, 535cm^{-1} with PED 64, 21, 36, 43, 11, 34, 33, 10, 11, 22, 43% respectively.

Modes	Wavelength cm^{-1}		I_{IR} [b]		I_{RAMAN} [c]		Assignments PED (%)
	Unscaled	Scaled[a]	Relative	Absolute	Relative	Absolute	
72	3052	2933	0	0	175	6	STRE CH(86)
71	3051	2932	10	6	0	0	STRE CH(86)
70	3031	2913	0	0	237	8	STRE CH(78)
69	3030	2912	42	26	3	0	STRE CH(86)
68	3027	2909	13	8	241	8	STRE CH(97)
67	3027	2908	60	37	54	2	STRE CH(92)
66	2922	2808	18	11	85	3	STRE CH(70)
65	2922	2808	13	8	118	4	STRE CH(70)
64	2913	2800	27	17	31	1	STRE CH(100)
63	2913	2800	4	2	229	26	STRE CH(99)
62	2853	2742	0	0	899	30	STRE CH(100)
61	2853	2742	80	49	2	0	STRE CH(100)
60	1859	1787	0	0	2983	100	STRE CC(64)
59	1654	1589	44	27	0	0	STRE CC(21)
58	1628	1565	0	0	19	1	STRE CC(36)
57	1623	1559	0	0	620	21	BEND CCC(23)
56	1617	1554	19	12	1	0	STRE CC(43)
55	1522	1463	163	100	0	0	
54	1509	1450	0	0	32	1	BEND HCH(44)
53	1504	1445	22	14	1	0	BEND HCH(57)
52	1502	1444	12	8	0	0	BEND HCH(64)
51	1502	1444	0	0	25	1	BEND HCH(77)
50	1464	1407	0	0	20	0	BEND HCC(28)+ BEND HCN(28)
49	1438	1382	0	0	86	3	BEND HCH(72)
48	1437	1381	0	0	1	0	BEND HCH(71)

47	1413	1358	19	12	0	0	BEND HCC(44)+ BEND HCN(14)
46	1410	1355	0	0	29	1	BEND HCC(22)
45	1338	1286	0	0	22	1	BEND HCN(40)
44	1309	1258	9	5	0	0	STRE CC(11)+STRE NC(39)
43	1287	1237	0	0	0	0	BEND HCC(22)+BEND HCN(32)
42	1265	1215	0	0	42	1	STRE CC(34)
41	1261	1212	0	0	188	6	STRE NC(42)
40	1259	1210	8	5	0	0	STRE CC(33)
39	1183	1137	9	5	0	0	BEND HCC(55)
38	1172	1126	0	0	10	0	BEND HCC(49)
37	1116	1072	3	2	0	0	TORS HCCC(54)
36	1116	1072	0	0	0	0	TORS HCCC(55)
35	1099	1056	19	12	0	0	STRE NC(20)
34	1080	1037	0	0	5	0	TORS HCCC(48)
33	1069	1027	29	18	0	0	TORS HCCC(50)
32	1064	1022	1	1	0	0	TORS HCCC(81)
31	1060	1019	4	2	0	0	TORS HCCC(58)
30	1060	1018	11	7	0	0	STRE CC(10)+BEND CCC(11)
29	1054	1013	0	0	11	0	STRE CC(11)
28	982	944	0	0	1	0	TORS HCNC(76)
27	981	943	0	0	0	0	TORAS HCNC(82)
26	927	891	1	1	1	0	TORS HCCC(79)
25	913	877	57	35	0	0	TORS HCCC(76)
24	864	830	0	0	187	6	
23	822	790	2	1	0	0	STRE CC(22)+BEND CCN(38)
22	773	742	0	0	3	0	TORS CCNC(16)+TORS CNCC(10)+OUT CCNC(14)
21	758	728	9	6	0	0	TORAS CCNC(32)+TORS CCCN(21)+TORS CNCC(12)+OUT CCNC(14)
20	724	696	0	0	2	0	STRE CC(43)+BEND CCC(25)
19	686	659	8	5	0	0	STRE CC(17)+BEND CCN(18)+BEND CNC(23)+BEND NCC(17)
18	654	629	0	0	15	1	BEND CCN(14)+BEND CNC(11)+BEND CCC(13)+BEND NCC(11)
17	557	535	5	3	0	0	STRE CC(24)+BEND CCC(12)
16	553	531	1	1	1	0	TORS CCCN(33)+OUT CCNC(22)
15	500	480	1	1	3	0	BEND CCN(22)+BEND NCC(22)+BEND CCC(22)
14	492	473	3	2	1	0	OUT CCCC(46)
13	447	429	0	0	1	0	TORS CCNC(28)+TORS CNCC(27)
12	425	408	9	6	0	0	TORS CCNC(26)+TORS CCCN(10)+TORS CNCC(26)
11	414	398	0	0	0	0	TORS HCCC(84)
10	407	392	0	0	3	0	BEND CCC(74)
9	394	379	2	1	0	0	TORS HCCC(21)+OUT CCCC(45)
8	332	319	0	0	7	0	
7	323	311	0	0	4	0	STRE CC(10)

6	310	214	0	0	2	0	BEND CCN(11)+BEND NCC(11)+BEND CCC(60)
5	268	257	0	0	0	0	TORS CCCN(23)+OUT CCCC(30)+OUT CCNC(12)
4	157	151	5	3	0	0	BEND CCN(36)+BEND NCC(36)
3	58	56	0	0	0	0	TORS CCNC(15)+TORS NCCC(15)+TORS CNCC(20)+OUT CCNC(20)
2	-35	-33	4	3	0	0	TORS NCCC(76)
1	-48	-46	0	0	1	0	TORS HCCC(14)+TORS CCNC(26)+TORS CNCC(26)+OUT CCNC(25)

Table 2: Theoretical vibrational frequency of abametapir.

a - scaling factor 0.961 for B3LYP/6-311++G (d, p) basis set.

b - Relative absorption intensities normalized with highest peak absorption equal to 100.

c – Relative Raman intensities normalized to 100.

UV absorption spectrum

UV absorption spectrum of Abametapir was Theoretically calculated using Time Dependent Density Functional Theory (TD-DFT) approach, utilizing B3LYP/6-311++G(d,p) as the basis set and the spectrum is shown in Figure 4. The formula E= hc/ λ was utilized to compute the band gap energy, where λ represents the cut-off wavelength and h stands for Planck's Constant and c for light velocity respectively [38,39]. Table 3 presented the UV-Visible spectral data. Theoretical wavelengths obtained for Abametapir was 310,294,292 nm with band gap energy 3.99,4.20,4.23eV respectively. Maximum band gap 4.23eV was obtained for the wavelength 292nm.

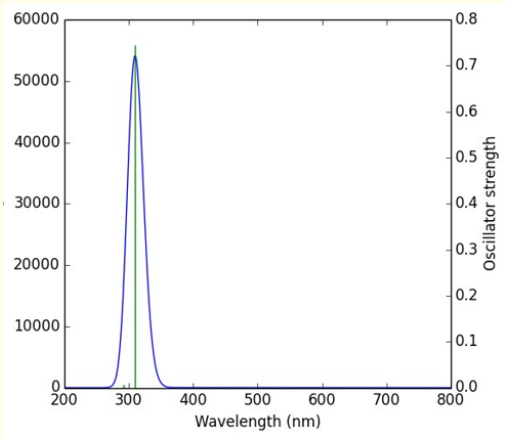

Figure 4: Theoretical UV-Visible Absorption Spectrum of Abametapir

Wavelength (nm)	Band gap(eV)	Energy	Oscillatory Strength	Symmetry	Assignments (Major and Minor contribution)
310	3.99	32251	0.7447	Singlet-A	HOMO->LUMO (97%)
294	4.20	33951	0.0002	Singlet-A	HOMO->L+1 (92%) H-3->LUMO (6%)
292	4.23	34182	0.0067	Singlet-A	H-1->LUMO (97%)

Table 3: Theoretically calculated electronic properties of abametapir using td-dft method.

Homo-lumo analysis

Molecular interactions with other Species are ascertained using the highest occupied molecular orbital (HOMO) and lowest unoccupied molecular Orbital (LUMO). Band gap energy or the energy difference between HOMO and LUMO is crucial in deciding the molecule's activity and chemical stability [40]. Gaussian Software was used to calculate the orbital energy gap and HOMO-LUMO energies at B3LYP/6-311++G(d,p). Title compound in relation to ionization potential (IP), electron affinity (EA), Electronegativity (χ), Chemistry hardness(ᵑ), Softness(S), Chemical potential(μ), and Electrophilic index (ω) are shown in Table 4. The simulated frontier molecule (FMO) is shown in Figure 5. The band gap energy (4.7721eV) determined from HOMO and LUMO agrees with the band gap energy (4.20eV) derived from the UV visible spectrum. Low softness value (0.2096) indicates that title compound is suitable for pharmaceutical applications.

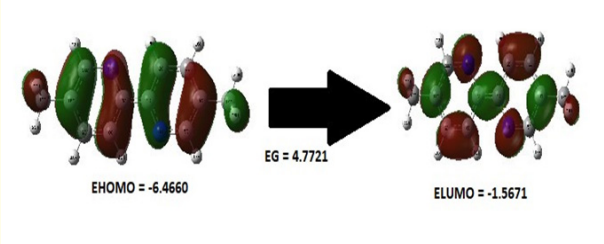

Figure 5: Atomic orbital HOMO-LUMO Composition of the Frontier Molecular orbital of Abametapir.

Properties	B3LYP/6-311++G(d,p)
HOMO(eV)	-6.3392
LUMO(eV)	-1.5671
Ionization potential	6.3392
Electron affinity	1.5671
Energy gap(eV)	4.7721
Electronegativity	3.9532
Chemical potential	-3.9532
Chemical hardness	2.3861
Chemical softness	0.2096
Electrophilicity index	3.2747

Table 4: Homo lumo calculated energy values of abametapir by B3LYP/6-311++G(d,p).

Electrophilic and nucleophilic analysis

MEP is a very helpful Descriptor for identifying places for electrophilic and nucleophilic reactions as well as Hydrogen bonding interactions. Molecular electrostatic potential is correlated with electron density. Mapping of molecular electrostatic potential is highly helpful in the examination of the molecular structure with its physicochemical property correlations [41]. DFT techniques was used to generate MEP map and it is displayed in Figure 6. There are two main sites: Nucleophilic sites, where the atoms are prepared to share electrons, and Electrophilic sites, where the atoms have a tendency to attract electrons. Electrophilic reactivity is associated with the negative regions (red colour) of MEP, while Nucleophilic reactivity is associated with the positive parts (blue colour). Neutral places are indicated by the green site on the map. MEP map of Abametapir shows that the Positive Potential sites are located around the Hydrogen atom, whereas Negative Potential sites are found on the Nitrogen atom. These active sites were discovered to be conclusive proof of biological activity inside the compound under study.

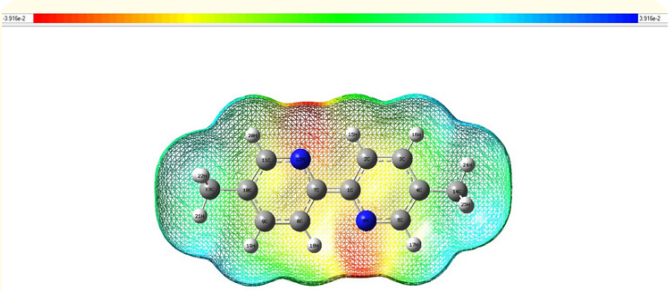

Figure 6: MEP Surface of Abametapir.

Topology analysis

Investigation conducted by ELF and LOL illustrates the likelihood of discovering an electron pair. LOL is a representation of the localised electron cloud, while ELF deals with electron pair density. The topological analysis of Abametapir was created and examined using the MULTIWFN 3.7 software [42]. Strong ELF values are indicated by the red zone, whereas weak ELF values are indicated by the blue zone. The main objective of studies on electron local fields (ELFs) is to understand the qualitative behaviour of electrons in a system. A red zone in LOL implies a higher Pauli repulsion, while a blue zone suggests a smaller Pauli repulsion [43]. Hydrogen Atoms H17, H20, H21, H24 of Abametapir shows high ELF and LOL values. While, carbon atoms C4, C5, C10, C11, C13, C14 of Abametapir shows low ELF and LOL values Figures 7 and 8 display the LOL and ELF diagrams.

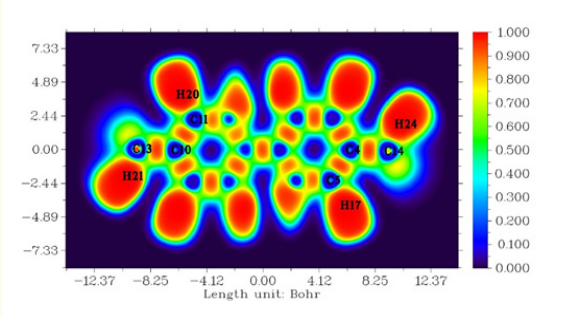

Figure 7: ELF Color filled Map of Abametapir.

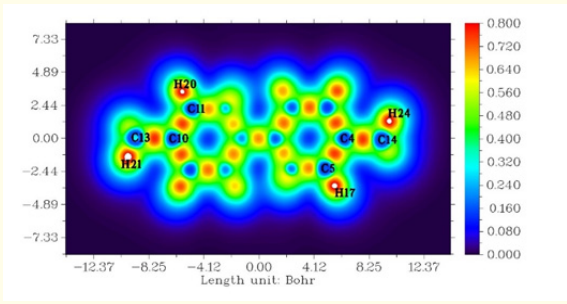

Figure 8: LOL Color filled Map of Abametapir.

Drug likeness

With the Swiss ADME web tool, ADME parameters such as absorption, distribution, metabolism, and excretion can be assessed. PubChem [44] is where the canonical format of the title compound was obtained. By feeding the canonical format of Abametapir to Swiss ADME, the drug likeness parameters are displayed and the results are mentioned in Table 5. HBD, HBA, Molecular refractivity, and rotatable bond values for Abametapir are 0, 2, 1, and 57.40, which are within the desired range. MlogP value for Abametapir is 1.49, which provides insight into the molecule's lipophilic nature. According to the research, Abametapir met the requirements of Lipinski's rule of five, indicating that it is an active pharmaceutical compound [45].

Descriptors	Optimal range	Values of the title compound
Hydrogen Bond Donor (HBD)	≤5	0
Hydrogen Bond Acceptor (HBA)	≤10	2
Molar Refractivity	40-130	57.40
MlogP	≤5	1.49
Number of rotatable bonds	≤10	1
Molecular weight g/mol	≤500g/mol	184.24g/mol

Table 5: Drug likeness parameters of abametapir.

Ramachandran plot

The first person to determine the allowed values for phi and psi was G.N. Ramachandran. Ramachandran plot, which is a two-dimensional graphic, can be used to visualize these allowed values. Plotted on the X and Y axis between phi and psi [46,47]. Figure 9 displays Ramachandran map of protein 1P30(Adenovirus). Figure shows that 12% of residues are in the prohibited area and 86% of residues are in the most preferred area. Since the majority of the residues are located in the allowed region, Protein 1P30 is a stable protein.

Molecular docking analysis

A molecular modelling method called docking which is used to forecast how a protein will interact with smaller molecules. Molecular docking is a significant method in structural Molecular biology and computer-assisted drug design. The ligand and water molecules present in the target proteins were removed by using the AutoDock tools' visual interface [48]. Docking parameters are noted in Table 6. In Figure 10, docking conformation is displayed. The calculated binding affinity of Abametapir for protein 1P30, which is associated with Adenovirus is -7.0 kcal/mol. Whereas, the common medication Cidofovir has a binding affinity value of -6.6kcal/mol. When comparing the binding affinity values of Abametapir and Cidofovir, Abametapir is significantly more effective against Adenovirus than Cidofovir, which is the standard medicine. Abametapir was also docked with lung cancer protein (1M17) and showed a better binding affinity of -7.5 kcal/mol than the standard drug Erlotinib [49], which has a binding affinity of -7.11 kcal/mol. According to this study, Abametapir may be used as a useful drug to treat Adenovirus infections as well as Lung cancer. However, animal and human trials should be carried out before making it a drug.

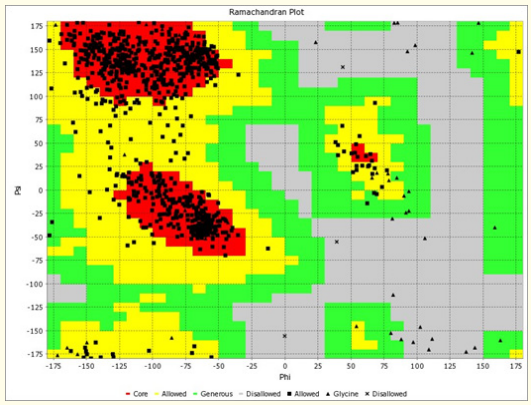

Figure 9: Ramachandran plot of 1P30 protein (Adenovirus).

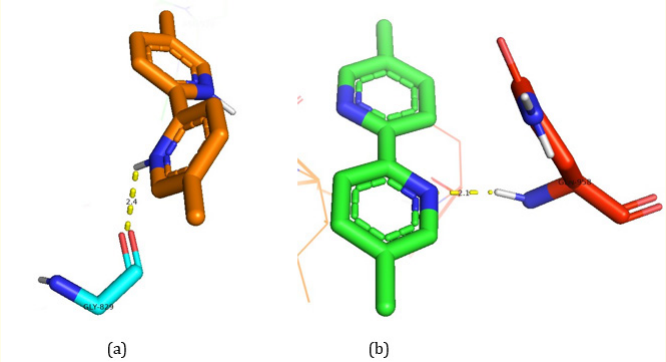

Figure 10: (a) Docking conformation of the ligand (Abametapir) with (a) 1P30 protein (Adenovirus) and (b) 1M17 protein (Lung cancer).

Protein	Compound name	Number of Hydrogen bonds	Bonded residue	Bond distance (Å)	Binding energy(Kcal\mol)
1P30 (Adenovirus)	Abametapir	1	GLY-829	2.4	-7.0
	Cidofovir (Standard drug)	4	GLN-821 LEU-819 VAL-828 LEU-831	2.6 2.3 2.7 2.3	-6.6
1M17 (Lung cancer)	Abametapir	1	GLN-958	2.1	-7.5

Table 6: Molecular docking parameters of abametapir.

Conclusion

Bond parameters offers insight into the stability of Abametapir and strength of the chemical bonds. Vibrational spectroscopy is a non-destructive identification method that measures the vibrational energy of Abametapir along with potential energy distribution values. UV absorption spectrum was Theoretically calculated using Time Dependent Density Functional Theory (TD-DFT) approach. The band gap energy (4.77eV) determined from HOMO and LUMO agrees with band gap energy (4.20eV) calculated from UV analysis. The title compound's MEP map shows that the Positive Potential sites are located around the Hydrogen atoms, whereas Negative Potential sites are found on the Nitrogen atoms. Local Orbital Locator (LOL) and Electron Localization Function (ELF) were created and investigated, the blue region represents low ELF values, whereas the red region represents high ELF values. SWISS ADME software used to obtain drug similarity parameters and it is noted that Abametapir satisfy all five rules. Ramachandran Plot is plotted for the protein 1P30 (Adenovirus) and it shows that 86% of residues are in the most favoured region. In Molecular docking the calculated Binding energy for the title compound is -7.0Kcal/mol which significantly exhibits better action against adenovirus than the Standard drug Cidofovir. Additionally, molecular docking analysis was carried out for lung cancer protein, which also shows very good binding affinity compared to the commercial drug (Erlotinib). From the above analysis, it can be predicted that Abametapir exhibits anti-viral and anti-cancer activity.

Bibliography

1. https://pubchem.ncbi.nlm.nih.gov/compound/Abametapir
2. Altaf., *et al*. "A review on the medicinal importance of pyridine derivatives". *Journal of Drug Design and Medicinal Chemistry* 1.1 (2015): 1-11.
3. Allaka Tejeswara Rao and Naresh Kumar Katari. "Synthesis of pyridine derivatives for diverse biological activity profiles: a review". *Recent Developments in the Synthesis and Applications of Pyridines* (2023): 605-625.
4. Savchenko V., *et al*. *Herald of the Russian Academy of Sciences* 80 (2010): 149-154.
5. Mashaly M M., *et al*. *Journal-Chinese Chemical Society Taipei* 51 (2004): 901-916.
6. Muthal N., *et al*. *Synthesis*. 2 (2010): 2450-2455.
7. Firke S., *et al*. *Asian Journal of Research in Chemistry* 2 (2009): 157-161.
8. Yang XT., *et al*. *Transition Metal Chemistry* (2011): 1-5.
9. Nassar E. *Journal of American Science* 6 (2010): 338-347.
10. Abele E., *et al*. "*Chemistry of heterocycliccompounds* 39 (2003): 825-865.
11. Vrabel M., *et al*. *European Journal of Inorganic Chemistry* (2007): 1752-1769.

12. Worachartcheewan A., *et al*. *Medicinal Chemistry Research* (2011): 1-9.

13. Lynch Joseph P., *et al*. "Adenovirus". In Seminars in respiratory and critical care medicine 32.4 (2011): 494-511.

14. Muruve DA. "The Innate Immune Response to Adenovirus Vectors*". Human Genetic Therapy* 15 (2004): 1157-1166.

15. Wold WSM., *et al*. "Fields Virology". 7th Lippincott, Williams and Wilkins; Philadelphia, PA, Baltimore, MD, USA: (2007): 1723-1740.

16. Renard G. "Adenoviral keratoconjunctivitis". *Journal Français d'Ophtalmologie* 33 (2010): 586-592.

17. Kuruvilla TK., *et al*. "Spectroscopic (FT-IR, FT-Raman), quantum mechanical and docking studies on methyl (3S)-3- (naphthalen-1-yloxy)-3- (thiophen-2-yl) propyl. Amine". *Journal of Molecular Structure* 1175 (2019): 163-174.

18. Rizwana B F., *et al*. "Spectroscopic investigation, hirshfeld surface analysis and molecular docking studies on anti-viral drug entecavir". *Journal of Molecular Structure* 1164 (2018): 447-458.

19. Manaa MR and Fried LE. "DFT and ab initio study of the unimolecular decomposition of the lowest singlet and triplet states of nitromethane". *The Journal of Physical Chemistry A* 102.48 (1998): 9884-9889.

20. Fathima Rizwana B., *et al*. "Spectroscopic investigation (FT IR, FT-Raman, UV, NMR), Computational analysis (DFT method) and Molecular docking studies on 2- (acetyloxy) methyl.-4- (2-amino-9h-purin-9-yl) butyl acetate". *International journal of Materials Science* 12 (2017): 196-210.

21. Sheela N R., *et al*. "Normal co-ordinate analysis, molecular structural, non-linear optical, second order perturbation studies of tizanidine by density functional theory". *Spectrochimica Acta Part A: Molecular and Biomolecular Spectroscopy* 139 (2015): 189-199.

22. Abraham CS., *et al*. "Quantum computational studies, spectroscopic (FT-IR, FT-Raman and UV-Vis) profiling, natural hybrid orbital and molecular docking analysis on 2, 4 Dibromoaniline". *Journal of Molecular Structure* 1160 (2018): 393-405.

23. Renuga S., *et al*. "FTIR and Raman spectra, electronic spectra and normal coordinate analysis of N, N-dimethyl-3-phenyl-3-pyridin-2-yl-propan-1- amine by DFT method". *Spectrochimica Acta Part A: Molecular and Biomolecular Spectroscopy* 127 (2014): 439-453.

24. Gnanasambandan T., *et al*. "Quantum Chemical and Spectroscopic (FT-IR, FT-Raman) Study, First Order Hyperpolarizability, NBO, Analysis HOMO and LUMO Analysis of Selegiline by abinitio HF and DFT Method". *Oriental Journal of Chemistry* 29.1 (2013): 185.

25. Uddin MA., *et al*. "UV-Visible spectroscopic and DFT studies of the binding of ciprofloxacin hydrochloride antibiotic drug with metal ions at numerous temperatures". *Korean Journal of Chemical Engineering* (2022): 1-10.

26. Zhang CR., *et al*. "DFT and TD-DFT study on structure and properties of organic dye sensitizer TA-St-CA". *Current Applied Physics* 10.1 (2010): 77-83.

27. MJ Frisch., *et al*. Gaussian 09, Revision D.01, Gaussian, Inc., Wallingford CT, (2016).

28. Roy D., *et al*. Semichem Inc., Shawnee Mission, Gaussview 6 (2016).

29. Zhurko GA., *et al*. "Chemcraft program, academic version 1.8; 2014". (2023).

30. Jamroz MH. Vibrational Energy Distribution Analysis: VEDA 4 Program, Warasaw, Poland (2014).

31. T Lu and F Chen. "Multiwfn: a multifunctional wavefunction analyze". *Journal of Computational Chemistry* 33.5 (2012): 580-592.

32. Daina., *et al*. "Swiss ADME: a free web tool to evaluate pharmacokinetics, drug-likeness and medicinal chemistry friendliness of small molecules". *Scientific Report* 7 (2017): 42717.

33. GM Morris., *et al*. "Automated docking using a Lamarckian genetic algorithm and an empirical binding free energy function". *Journal of Computational Chemistry* 19 (1998): 1639-1662.

34. Dassault Systems BIOVIA: Discovery studio visualizer 21.1.0.20298 (2020): 2021.

35. Jomroz MH. "Vibrational energy distribution analysis". VEDA4, Warsaw (2004).

36. Fathima Rizwana B., *et al*. "Spectroscopic investigation (FT-IR, FT-Raman, UV, NMR), Computational analysis (DFT method) and Molecular docking studies on 2- (acetyloxy) methyl.-4-(2-amino-9h-purin-9-yl) butyl acetate". *International Journal of Materials Science* 12.2 (2017): 2017.

37. Clara T., *et al*. "Structural, optical, thermal, dielectric and Z-scan study on novel (2E)-1- (4-aminophenyl)-3-(4-benzyloxyphenyl)-prop-2-en-1-one (APBPP) chalcone crystal for nonlinear optical applications". *Optical Materials* 109 (2020): 110331.

38. PK Chattaraj and B Maiti. "Philicity: A unified treatment of chemical reactivity and Selectivity". *The Journal of Physical Chemistry A* 107 (2003): 4973-4975.

39. Jebapriya J., *et al*. "Growth and characterization of a cyclohexanone based chalcone crystal 2 (E)- (4-N, N-dimethylaminobenzylidene)-5-methylcyclohexanone for nonlinear optical applications". *Optical Materials* 107 (2020): 110035.

40. George Jacob., *et al*. "Evaluation of vibrational, electronic, reactivity and bioactivity of propafenone—A spectroscopic, DFT and molecular docking approach". *Chemical Data Collections* 26 (2020): 100360.

41. E Tomasi J. "Electronic molecular and biomolecular spectroscopy". 226 (2020): 117614.

42. AD Becke and KE Edgecombe. "A Simple measure of electron localization In atomic and molecular systems". *The Journal of Chemical Physics* 92.9 (1990): 5397-5403.

43. Savin A., *et al. Angewandte Chemie International edition in englis*. 31.2 (1992): 187-188.

44. https://pubchem.ncbi.nlm.nih.gov/compound/Abametapir

45. Blum Lorenz C and Jean-Louis Reymond. "970 million drug-like small molecules for virtual screening in the chemical universe database GDB-13". *Journal of the American Chemical Society* 131.25 (2009): 8732-8733.

46. RWW Hoff C and Sander G. Vriend- bioinformatics, 1997, EE Abola nature 381.6508 272-272.

47. E Krieger., *et al*. *Structure, Function and Bioinformatics* 47.3 (2002): 393-402.

48. A Dias., *et al*. "Polymer as Resides in the PA subunit nature". 458 (2009): 914-918.

49. Clara T Hannah., *et al*. "Quantum mechanical, spectroscopic and docking studies of (2E)-1- (4-aminophenyl)-3-(4-benzyloxyphenyl)-prop-2-en-1-one Chalcone derivative by density functional theory-A prospective respiratory drug". *Materials Today: Proceedings* 50 (2022): 2816-2825.